Technical Report 120

FEBRUARY, 1965

Excavations in Frozen Ground Alaska, 1960-61

by

J. E. McCoy

U.S. ARMY MATERIEL COMMAND
COLD REGIONS RESEARCH & ENGINEERING LABORATORY
HANOVER, NEW HAMPSHIRE

Technical Report 120
FEBRUARY, 1965

Excavations in Frozen Ground Alaska, 1960-61

by
J. E. McCoy

U.S. ARMY MATERIEL COMMAND
COLD REGIONS RESEARCH & ENGINEERING LABORATORY
HANOVER, NEW HAMPSHIRE

PREFACE

This is a report on tests of explosives for excavating frozen ground, Task 5010.02209, a part of research conducted by the Applied Research Branch, U. S. Army Cold Regions Research and Engineering Laboratory (USA CRREL). The tests were conducted in frozen silt near Fairbanks, Alaska, from 15 December 1960 to 20 April 1961.

This report was prepared by J. E. McCoy, Project Leader. Other personnel participating in the tests were: J. V. Tedrow and R. W. Wendler, of USA CRREL, and W. K. Boyd, Technical Director, USA CRREL. Mr. R. W. Wallstedt, Lawrence Radiation Laboratory, visited the U. S. Army, Alaska, Yukon Command, the Alaska District, Corps of Engineers, Ft. Wainwright Plant and Equipment Facility, and Lawrence Radiation Laboratory. All explosive charges were cast at Picatinny Arsenal. The Lawrence Radiation Laboratory contributed funds for providing the two 2560-lb spherical charges.

CONTENTS

ILLUSTRATIONS

TABLES

SUMMARY

Spherical and cylindrical charges of 1, 4, 8, 32, 256 and 2560 lb were exploded in frozen silt near Fairbanks, Alaska, to investigate the applicability of lambda scaling for placing charges in frozen ground. One hundred and thirty holes, ranging from 3 to 6 in. in diameter, and 2 to 6 ft in depth, were drilled with a truck-mounted core drill. Compressed air, passed through an air-to-air heat exchanger to cool it below 25°F, was used as a drilling fluid. Charge emplacement, stemming, and detonation are also described. Six basic series were fired which, except for the 2560-lb shots, consisted of two spheres and two cylinders buried at each of six scale depths. The crater volume was calculated by the centroid-volume method. A planimeter was used to measure the area of two mutually perpendicular cross sections through the center of the blast hole. Upon detonation of charges of a given weight at increasing depths, the resultant crater will increase to a maximum and rapidly drop off and disappear. At depths slightly beyond optimum, lambda scaling does not apply and the results are indeterminate.

EXCAVATIONS IN FROZEN GROUND — ALASKA, 1960-61

by

J. E. McCoy

INTRODUCTION

Spherical and cylindrical charges of 1, 4, 8, 32, 256 and 2560 lb were exploded in frozen silt near Fairbanks, Alaska. The objective was to investigate the applicability of lambda (λ) scaling for placing charges in frozen ground. (Lambda, in feet, is equal to the cube root of the charge weight in pounds.) The effect of the shape of the charge was also investigated. Spheres and cylinders with a height to diameter ratio of 4 to 1 were used in these experiments.

DEFINITIONS

The following definitions will be used:

λ, lambda — The cube root of the charge weight in lb; i.e., an 8-lb charge buried at 2.5 lambda would have its center of gravity 5 ft beneath the surface.

Apparent crater — Size of the crater as it appears to an observer immediately after the blast.

True crater — Size of the crater which can be excavated with a clamshell and/or pick and shovel after the blast.

d_c — Depth to the center of gravity of the charge in ft.

h_c — Depth of the true crater in ft.

Critical depth — Minimum depth at which all the energy of the blast is contained without breaking the surface.

Optimum depth — Depth at which the blast does the greatest amount of usable work, i.e., creates the maximum true crater.

SITE SELECTION AND PREPARATION

Preliminary reconnaissance and exploratory drilling in the spring of 1960 led to the selection of a site in the U. S. Army Yukon Command Maneuver Area, approximately 7 miles north of Eielson AFB. The site was relatively flat and covered with the stunted black spruce typically found over permafrost in this region. The material was uniform silt frozen (Vr, s) to a depth of 65 ft. Gradation curves are presented in Figures B1 and B2 for core samples obtained at two locations in the test area. The depth, wet and dry density, moisture content, organic content, specific gravity, and a verbal description of the soil is given in Table BI, and typical core samples are shown in Figure B3.

An access road $1\frac{1}{2}$ miles long was constructed during the first 2 weeks of December 1960 between the existing road net and the test site. After being smoothed with a road grader, the road remained in good condition until the spring breakup. The camp, constructed in mid-December, consisted of two Jamesway huts, an explosives magazine, and a motor-pool area. One Jamesway was used as the project office and as quarters for two watchmen; the other was used as a mess hall and for indoor storage. Approximately 52 acres were cleared of brush.

FIELD PROCEDURE

Drilling of charge holes

One hundred thirty holes, ranging from 3 to 6 in. diam and from 2 to 6 ft deep, were drilled with a truck-mounted core drill. Compressed air, passed through an air-to-air heat exchanger to cool it below 25F, was used as a drilling fluid. (The fluid was cooled to insure that the soil remained frozen; thawed soil would plug the bits, cause the cuttings

to stick to the wall of the hole, and build up on the drill string.) An ambient temperature of below 20F was required for effective operation of the heat exchanger.

The larger diameter holes were drilled with a Williams LDH50 auger using bits with tungsten-carbide inserts.* Eighty holes from 8 to 48 in. in diam and up to 49 ft in depth were dug. A tractor with a 1-yd front-loading scoop was used to take the spoil from the auger.

Charge emplacement

Three-eighths-inch holes were provided through the center of each charge so that Primacord could be used as a detonator. For charges up to 32 lb the Primacord was strung through the hole and used to lower the charge into position. The 256-lb cylinders and the five 512-lb cylinders which made up each 2560-lb cylinder had eyebolts cast into them so that the charge could be lowered by ropes, which could then be recovered. The 256-lb spheres were lowered with a specially made $\frac{3}{4}$-in. rope sling that resembled a cargo net. The sling was not recovered. The 2560-lb spheres were tightly strapped onto a ring for safe removal from the casting-shipping mould. The same ring and straps were used to lower the charge into position. A positive acting winch (32,000-lb capacity) was used to lower all charges weighing over 32 lb (see Fig. 1).

Stemming

A mixture of ash and gravel was used for stemming. The material was mixed with 24% water, tamped securely into the hole, and then allowed to freeze-back for from 4 to 14 days, depending on ambient temperature, hole diameter, and depth. Some of the 256-lb charges were stemmed in 2-ft increments and 3 days allowed between lifts to assure complete freeze-back. However, no increase of stemming effectiveness was noticeable where this method was employed. The 2560-lb spheres were covered to a depth of 2 ft with damp ash, which was allowed to freeze for 5 days. The remainder of the hole was then filled with pit-run gravel which held successfully. Some stemming failures were noticed in the shots up to 32 lb. The failures seemed to be caused when the Primacord, which was detonated by a cap from the surface, broke the adfreeze bond between the stemming and the hole wall. This allowed the stemming to be ejected in a large piece similar to a slug from a gun barrel. The application of a layer of dry gravel, with a thickness approximately twice the diameter of the hole, at one-half the charge depth appeared to solve the problem.

Detonation

Each charge was designed to be detonated by Primacord strung through the center of the charge. The Primacord was extended approximately 1 ft above the ground surface to allow an Engineer Special Electric Blasting Cap to be attached to the cord.

To insure safety and positive detonation secondary detonators were installed with the 256- and 2560-lb charges. Each of the secondary detonators consisted of ten $\frac{1}{4}$-lb sticks of 60% dynamite wrapped into a bundle with four wraps of Primacord and lowered by the Primacord into direct contact with the main charge. Two secondary detonators were buried with each 256-lb charge and four were buried with each 2560-lb charge. The secondary systems were required and successfully utilized when misfires in the primary detonation systems were experienced with two 256-lb and one 2560-lb charge. A misfire was also experienced with one 32-lb charge which was disposed of with a 15-lb M2A3 shape charge.

TESTS

Six basic series weighing 1, 4, 8, 32, 256, and 2560 lb were fired. Except for the 2560-lb shots, each series consisted of two spheres and two cylinders buried at each of six scaled depths of 1.0, 1.5, 2.0, 2.25, 2.5, and 2.75 λ. The 2560-lb series, two spheres and four cylinders, were buried at 1.75, 2.0, 2.5, 2.75, 3.0, and 3.2 λ. Additional shots were fired when necessary to pinpoint critical depth and to clarify ambiguous results.

---

*See SIPRE Special Report 38, Performance of a Williams auger in permafrost.

Figure 1. Placing 2560-lb spherical charge.

Immediately after a charge was fired, the resultant crater was cross sectioned, on two mutually perpendicular axes through the center of the shot hole, to determine the apparent crater. The crater was then excavated to expose the true crater. After the true crater had been completely cleaned out, it was again cross sectioned on two mutually perpendicular axes through the shot hole.

The craters resulting from explosion of the 2560-lb charges were not excavated.

CALCULATION OF CRATER VOLUME

The crater volume was calculated by the centroid-volume method. A planimeter was used to measure the area of two mutually perpendicular cross sections through the center of the blast hole, called cross sections A and B. The cross sections were then split along the centerline of the drill hole, and the distance (centrodial radius) from the centerline of the drill hole to the centroids of the right-half and left-half of cross section A was averaged. The same measurements and average were determined for cross section B. The crater volume is then computed:

$$V = \frac{V_a + V_b}{2} = \text{Crater volume}$$

$$V_a = \pi \bar{R}_a A_a = \text{Crater volume from cross section A}$$

$$V_b = \pi \bar{R}_b A_b = \text{Crater volume from cross section B}$$

where

$\bar{R}_a$ = Average centrodial radius of cross section A

A_a = Area of cross section A

$\bar{R}_b$ = Average centrodial radius of cross section B

A_b = Area of cross section B.

Data sheets which show the complete crater data for each shot are enclosed (App. A).

RESULTS

Applicability of lambda scaling

True crater volume. The data show that, as a series of charges of a given weight are detonated at increasing depths of burial, the resultant true crater will increase to a maximum and rapidly drop off and disappear completely. If crater volume per pound of charge is plotted on semi-log paper vs depth of charge in lambda (Fig. 2), two separate phenomena are evident. At burial depths between 1λ and optimum, which is about 2.5 λ in frozen silt, the data plot as a straight line. Though the charges varied in size from 1 to 256 lb, they all followed this single straight line. Therefore, lambda scaling does apply between 1 λ and optimum. There is no reason to suspect any variation from lambda scaling at depths less than 1 λ, though this range is predominantly characterized by much noise and air blast and was not investigated during this project.

At depths slightly beyond optimum, lambda scaling does not apply and results are indeterminate. An increase in the burial depth of just 0.25 λ beyond optimum may have any of these results: the crater may be much smaller; there may be no crater at all; or a few shots may result in a crater actually larger than what was originally thought to be optimum. An increase in burial depth beyond this 0.25 λ will result in a below-critical-depth shot and there will be no damage other than a slight doming or a few cracks showing on the ground surface. The effect of a blast can, therefore, be predicted reliably up to the optimum depth and at depths beyond critical.

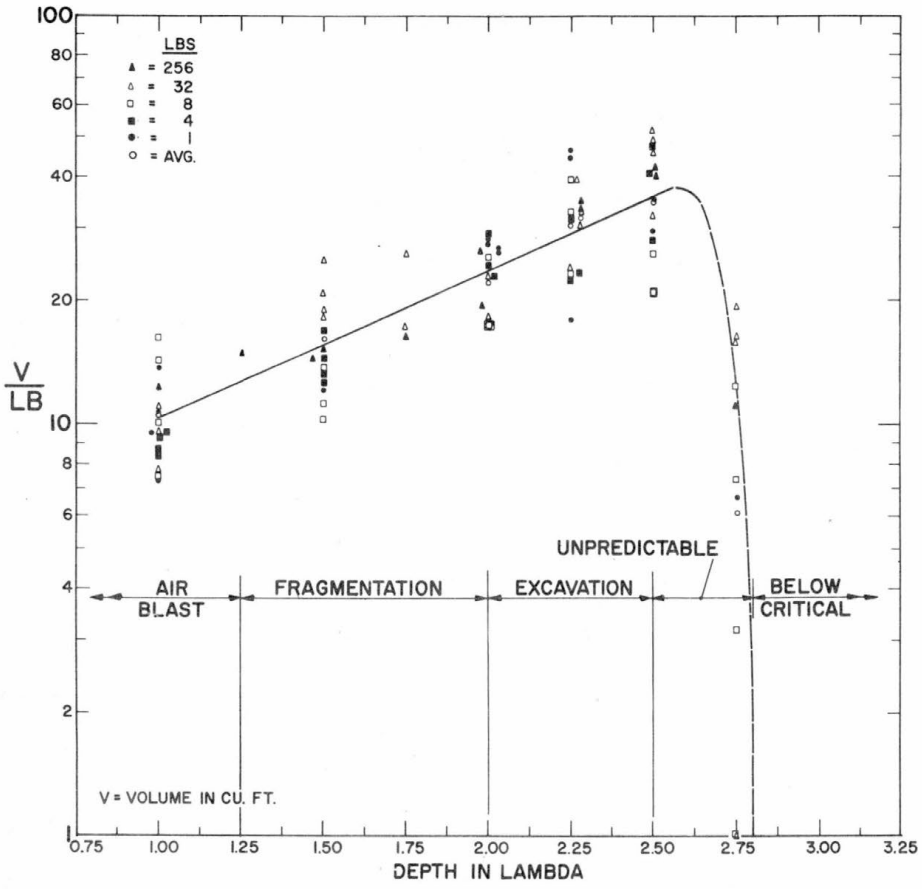

Figure 2. Volume utilization curve, true crater in frozen silt. Showing ranges of similar behavior.

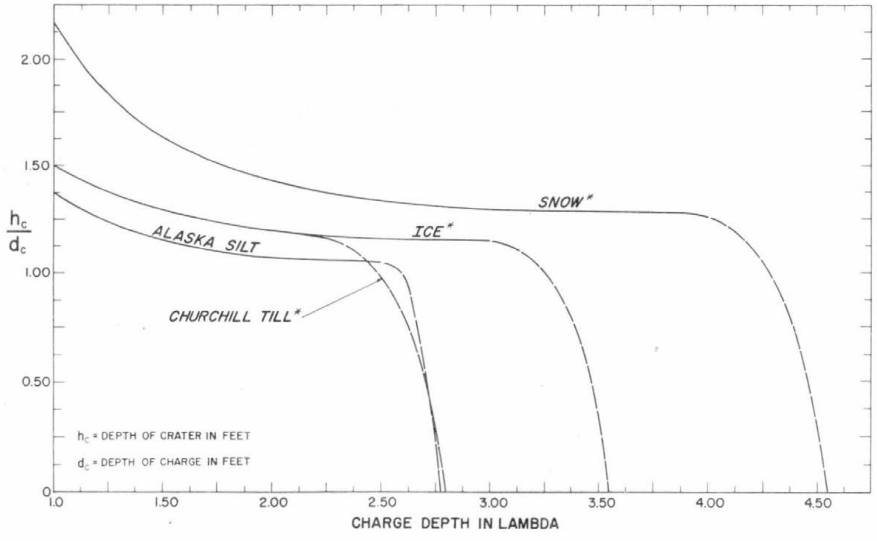

Figure 3. True crater depth ratio vs charge depth. Average values. Curves based on data obtained by Livingston (see App. C).

The narrow, approximately 0.25 λ range between optimum and critical depths has been indeterminate in all field work. There are several possible reasons for this inconsistency: (1) In nature it is impossible to find a true isotropic, homogeneous solid medium to work in. (2) Perfect stemming containment, center detonation, and instantaneous equal-energy release per pound of explosive detonated is seldom achieved under field conditions. These parameters are always present and account for some of the inherent scatter in field data. When the depth of burial is close to critical and the material is stressed to its maximum without failure, slight variations in the parameters will have a great effect on the results.

True crater depth. The depth-ratio curve (Fig. 3) shows that, as the depth of burst increases, the crater depth will more closely approximate the depth of the charge. When optimum depth has been reached, the depth of crater will be maximum; a slight increase in charge depth beyond optimum will cause a very rapid decrease in the depth of crater which can be excavated. This curve shows that lambda scaling is valid for predicting the depth of a true crater up to optimum but the depth range between optimum and critical is indeterminate.

Apparent crater volume. Volume utilization curves (Fig. 4) were plotted for the apparent crater in an attempt to discover a relationship with lambda scaling. The preliminary curve for the 2560-lb shots is based on a study of the motion pictures and the experience gained in the field during the project. The graphs show that, unlike the true crater, there is no particular lambda-scaled depth at which a maximum size crater is consistently obtained, i.e. optimum, or no crater is obtained at all, i.e. critical. It was noticed that there was a definite trend for optimum-size apparent craters to be produced from lower scaled depths as the charge weight increased. The observations made and the motion pictures taken show that proper stemming confinement is not only more difficult to achieve for shallow shots, but will also have a greater effect on the apparent crater than on the true crater. Poor stemming confinement may cut the size of the apparent crater by 75%, while it will only lower the size of the true crater by a factor of 10 to 15%. The graph indicates that, for the larger charges, the largest apparent crater will occur at some depth less than 1 λ.

Effect of charge shape

Field observations, motion pictures, and study of the craters and data (Fig. 5) show that, contrary to previous beliefs, the sphere is not greatly more efficient than the cylinder. In the blasts between 1 λ and 2.25 λ there was no indication that either shape was more efficient. At the optimum depth of 2.5 λ, the cylinders showed less scatter and were 17.4% more efficient.

Practical considerations of lambda scaling

There are several ranges of similar behavior which can be selected and utilized to predict the results of a crater burst. These ranges are shown on the volume utilization curve for Alaska frozen silt (Fig. 2). Of course, all predictions are dependent upon the stemming being securely tamped and holding the blast energy efficiently. The first range, characterized by excessive air blast and noise, covers depths from the surface to 1.25 λ. Small particles weighing less than 2 lb may travel up to 800 ft horizontally. The second range, the fragmentation range, covers the depths from 1.25 to 2.0 λ. This range is characterized by considerable waste of energy in throwing flyrock into the air and breaking the material into small pieces. The material which can be excavated will average between 0.75 and 1.0 cu ft. Pieces weighing 2 to 4 lb may travel 600 ft horizontally. The next range, the excavation range, between 2.0 and 2.5 λ, utilizes nearly all the energy in breaking the frozen silt into manageable pieces. The majority of the pieces will be between 1.0 and 2.5 cu ft. Noise and flyrock will have been greatly diminished though 4- to 5-lb pieces may be thrown 450 ft horizontally. The fourth relatively narrow range, between 2.5 and 2.75 λ, can best be called the unpredictable range. Flyrock may be similar to the excavation range, but this unpredictable range should not be considered when the production of a true crater is important. The fifth and last range is the depth of burial beyond critical, which will only result in a camouflet and no disturbance to the surface. It also is of little use in excavation work.

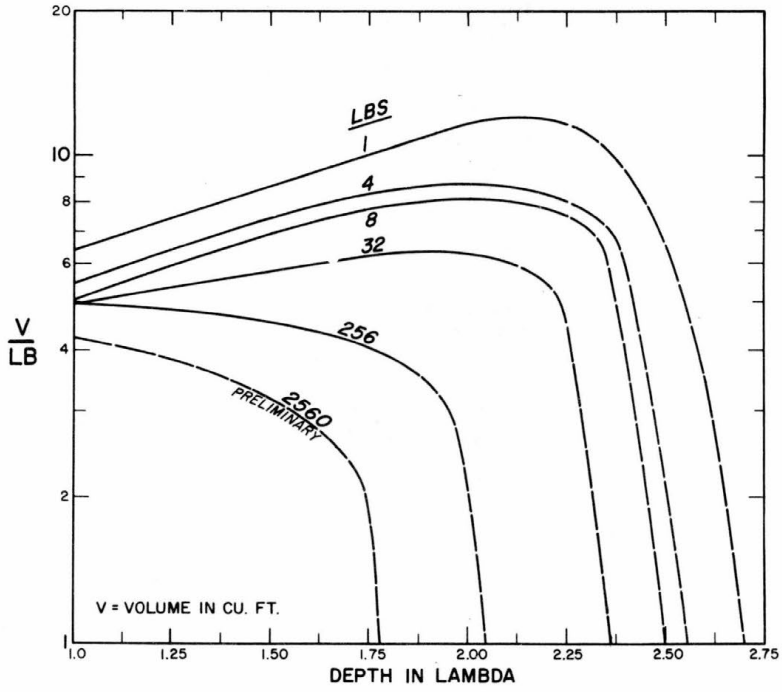

Figure 4. Volume utilization curve, apparent crater in frozen silt. Average values for given charge weights.

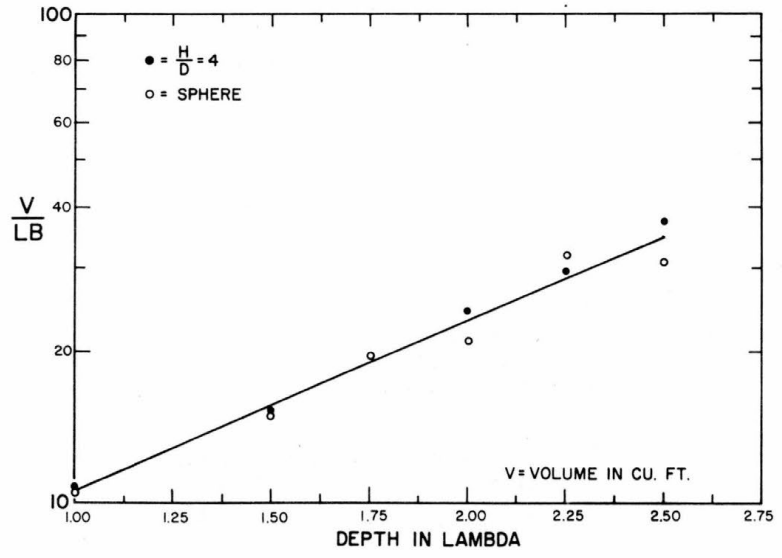

Figure 5. Effect of charge shape, true crater in frozen silt. Average values of all data.

It should be noted that the particle sizes mentioned are necessarily only approximate and are intended to give a rough idea of the expected results. Occasionally a particle may be much larger than the expected average. The truck-mounted $\frac{1}{2}$-yd cranes had no difficulty in excavating to the true crater in all the 32- and 256-lb blasts.

The horizontal distance the flyrock will travel is quite unpredictable, but the figures given are based on observation of several hundred blasts. The limit for observers would be approximately twice the distances mentioned, to insure safety, though it was noted that 1000 ft would have been a safe distance regardless of the weight of the charge detonated. It appears that the weight of charge is not the prime consideration for the distance that flyrock will travel. The air resistance of the rough flyrock seems to stop it quickly, regardless of its initial velocity. In any blast, one or two small pieces will usually travel twice as far as the majority of the flyrock. Therefore, even at the above-mentioned distances it behooves an observer to stay alert.

Example and use of lambda scaling

The volume utilization graphs for a true crater can be used to predict either the volume of a true crater which can be expected from a given weight of charge at any depth or, conversely, the depth at which a given weight of charge must be placed to effectively utilize its blast energy.

The depth-ratio curve (Fig. 3) can be used to predict the depth of a true crater which will result from any weight of charge or depth of burst over the depth range from 1 λ to 2.5 λ.

If a small cratering charge of known weight is detonated at a known depth, it is possible, by using lambda scaling, to predict the effects of a much larger charge at the same scaled depth. For simplicity, let us consider two charges weighing 8 lb and 27 lb, respectively. If we bury the 8-lb charge at a d_c of 4 ft, which is 2 λ ($4 = 2\sqrt[3]{8}$), the volume utilization curve shows that we can expect a true crater of 24 ft^3/lb or approximately 190 ft^3. If we then bury the 27-lb charge at the same scaled depth of 2 λ, d_c will be 6 ft ($2\sqrt[3]{27}$); we still expect to obtain a true crater of 24 ft^3/lb or 650 ft^3. The true-crater depth-ratio curve shows that the depth of the crater should be 1.055 times the depth of the charge or 4.2 and 6.3 ft, respectively.

Table I shows the results of 11 cratering shots, buried at the same scaled depth of 2.25 or 2.3 λ. Charge weight varied from 4 to 256 lb. From the volume utilization curve (Fig. 2), volume would be approximately 29 ft^3/lb and the depth ratio would be 1.05 (Fig. 5). The averages of all the data were approximately 106.5% of the expected values. This shows that our volume utilization curve is a little low, but inspection proves that a straight line is the best average which can be drawn, considering all the shots that were fired in the Alaska silt.

Comparison with other data

An attempt was made to compare the data obtained in the frozen Alaska silt with data obtained by Mr. C. W. Livingston under contract with SIPRE (App. C).* This contract work utilized various explosives in Greenland ice, Greenland snow, and Ft. Churchill frozen till. Volume utilization curves based on all the available data are shown (Fig. 6-8). It is noted that different types of explosives gave slightly different slopes to the straight line through the data for each material. The scatter, which is inherent to explosive cratering work, makes it almost impossible to separate the effects of each explosive type. Many more shots would be required to define the effect of each type of explosive on each of the several media.

Though the data are insufficient, there were no indications that lambda scaling was invalid over the ranges of weight and explosive types investigated. An average composite curve for each material was drawn to show the best possible approximation of the reaction of each material to explosive cratering (Fig. 9). Once again, it is shown that lambda scaling is valid only up to the optimum depth.

---

*From SIPRE Technical Report 30, Pt. II (1959), Technical Report 71 (1960), and Technical Report 86 (unpublished).

Table I. Results of lambda scaling, true crater in Alaska silt.

No.	Wt (lb)	d_c, Depth of charge (ft)	λ	Vol (ft^3)	Vol / (lb)	h_c, Depth of crater (ft)	$\frac{h_c}{d_c}$	% of given curves Vol / lb	% of given curves $\frac{h_c}{d_c}$
2.25λ from curve					29		1.05	100.00%	100.00%
5	256	14.6	2.3	8660	33.8	14	.96	116.0	91.0
12	256	14.6	2.3	8250	32.1	22	1.5	111.0	143.0
26	32	7.1	2.25	1084	33.9	8.2	1.15	116.0	109.0
27	32	7.1	2.25	775	24.2	8.3	1.17	84.0	112.0
40	32	7.3	2.3	1094	34.2	7.9	1.08	118.0	103.0
41	32	7.3	2.3	966	30.2	7.6	1.04	104.0	99.0
54	8	4.5	2.25	178	23.3	4.2	0.935	81.0	89.0
63	8	4.5	2.25	271	33.9	5.1	1.13	116.0	108.0
64	8	4.5	2.25	318	39.8	4.4	0.98	137.0	94.0
78	4	3.6	2.25	94	23.5	3.8	1.05	81.0	100.0
79	4	3.6	2.25	127	31.8	4.5	1.25	110.0	119.0
							Average	106.72	106.09

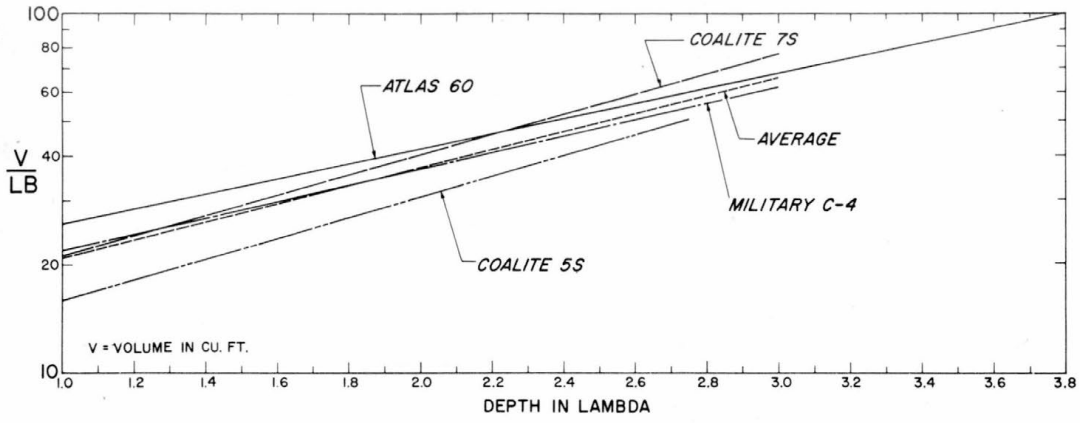

Figure 6. Volume utilization curves, true crater in ice, Greenland Ice Cap.

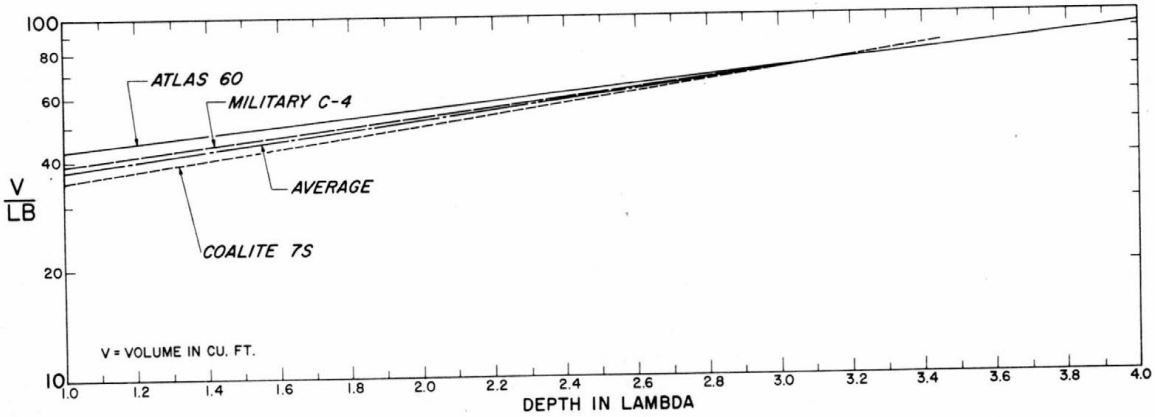

Figure 7. Volume utilization curves, true crater in snow, Greenland Ice Cap.

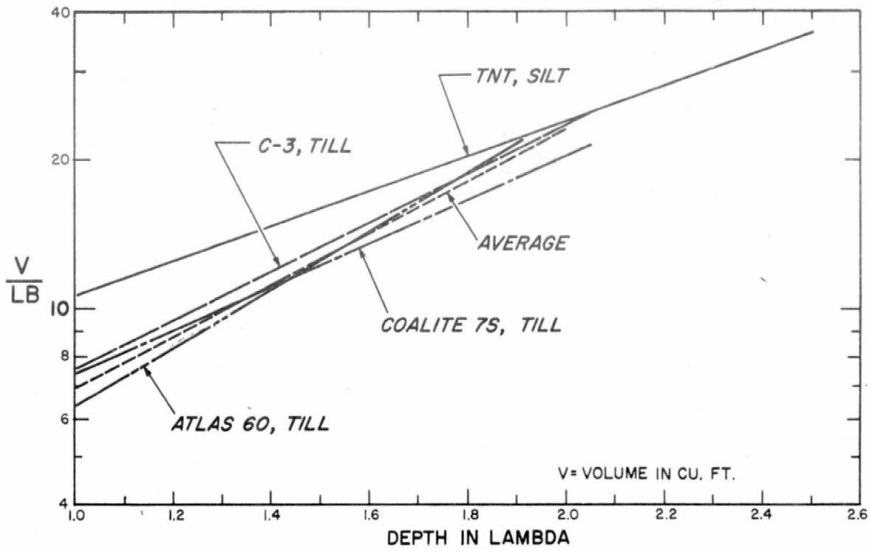

Figure 8. Volume utilization curves, true crater in frozen silt and till.

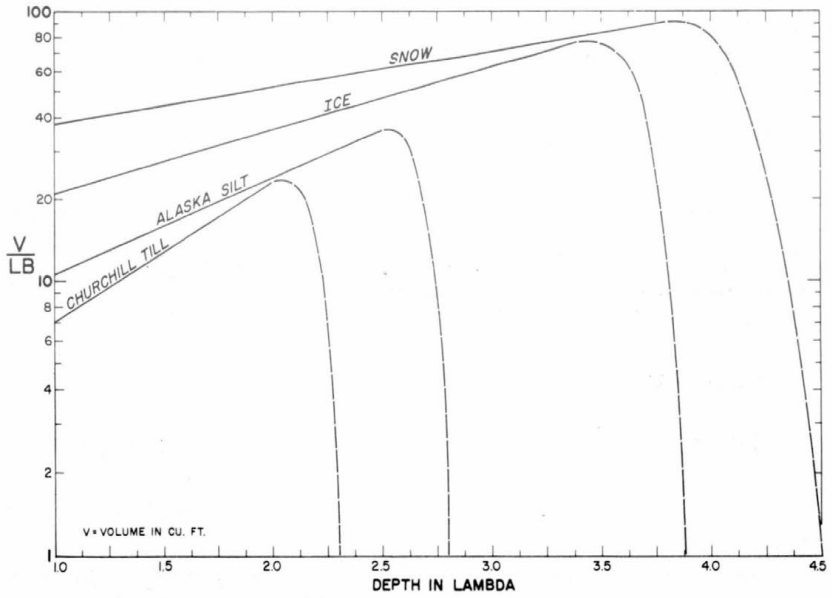

Figure 9. Composite volume utilization curves, true crater.

APPENDIX A: Crater data — Frozen silt, Fairbanks, Alaska.

Charge data			Apparent crater data										True crater data									
Shot no.	Depth (λ)	Depth (ft)	Area (ft²) N-S	Area (ft²) E-W	Vol (ft³)	Vol lb	Diam (ft)	Diam (λ)	Diam lb	Depth (ft)	Depth (λ)	Depth lb	Area (ft²) N-S	Area (ft²) E-W	Vol (ft³)	Vol lb	Diam (ft)	Diam (λ)	Diam lb	Depth (ft)	Depth (λ)	Depth lb	h_c/h_d
Wt = 256 lb H/D = 4																						
1	1.0	6.35	101.0	145.8	1598	6.2	22	3.46	.086	8	1.28	.031	175	172	3140	12.3	31	4.89	.121	8.5	1.34	.033	1.34
2	1.25	7.95	88	71	1071	4.2	22	3.46	.086	5	.079	.019	227	203	3835	15.0	32	5.05	.125	12	1.79	.047	1.50
3	1.45	9.2	15.6	14	93.5	0.37	11	1.73	.043	2	.031	.007	221	209	3760	14.7	32	5.05	.125	11.5	1.81	.045	1.25
4	1.95	12.4	41	42	715	2.8	27.5	4.33	.107	2.3	.036	.009	356	294	6830	266	38	6.0	.148	15	2.37	.059	1.21
5	2.3	14.6	No apparent crater (NAC)										404	347	8660	33.8	42	6.62	.164	14	2.21	.055	.96
6	2.5	15.9	NAC										387	419	10,700	41.7	44	6.93	.182	13	2.05	.051	.82
7	2.75	17.5	NAC										455	471	10,700	41.7	42	6.62	.164	19	3.0	.074	1.09
8	2.9	18.4	CRITICAL																				
Spherical																						
9	1.5	9.5	70	63	358	1.4	23	3.63	.090	4	.063	.015	211	210	3950	15.4	30	4.73	.118	11	1.73	.043	1.16
10	1.5A	9.5	33	55	948	3.7	29	4.56	.113	2.5	.039	.009	249	241	4660	18.2	32	5.05	.125	11.5	1.81	.045	1.21
11	1.95	12.4	NAC										251	316	4990	19.5	32	5.05	.125	15	2.37	.059	1.20
12	2.3A	14.6	36	42	401	1.6	18	2.84	.070	3.7	.058	.014	356	422	8250	32.1	36	5.68	.140	22	3.47	.086	1.50
13	2.3	14.6	NAC										227	178	3948	15.4	35	5.50	.137	12	1.79	.047	.82
14	2.5	15.9	NAC										444	451	10,370	40.4	42	6.62	.164	17.5	2.76	.068	1.1
15	2.8	17.8	31.2	37.9	322	1.3							131	132	2010	7.9	30	4.73	.118	10	1.57	.039	.56
16	2.8A	17.8	NAC										CAMOFLET										
17	1.5	9.5	38.5	54.5	726	2.8							221	214	3170	12.4	26	4.10	.101	12	1.79	.047	1.2
18	1.75	11.1	60	64	1210	4.7	28	4.41	.110	3.0	.048	.011	195	289	4200	16.4	30	4.73	.118	12	1.79	.027	1.08
19	2.75	17.5	44	33	353	1.4	12	1.89	.047	3.5	.055	.013	147	215	2920	11.4	23	3.63	.090	7	1.10	.027	.4
Wt = 32 lb H/D = 4																						
20	1	3.2	23.6	24.0	155	4.8	12	3.76	.376	3.4	.106	.106	26.8	25.6	311	9.7	15.5	4.85	.485	4.0	1.25	.125	1.25
21	1A	3.2	24.4	25.0	160	5.0	12.4	3.88	.388	4.0	1.25	.125	31.8	25.3	254	7.9	16.2	5.06	.506	3.4	1.06	.106	1.06
22	1.5	4.75	21.9	22.6	162	5.1	13.0	4.07	.407	2.75	.86	.086	66.4	58.9	608	19.0	18.0	5.64	.564	6.2	1.94	.194	1.30
23	1.5A	4.75	38.8	39.9	348	10.9	16.0	5.0	.50	4.0	1.25	.125	56.3	65.1	660	20.6	20.0	6.26	.626	5.8	1.82	.182	1.22
24	2	6.4	22.4	19.1	197	6.2	16.2	5.06	.506	2.7	.84	.084	79.8	73.5	599	18.7	19.0	5.95	.595	6.4	2.0	.20	1.0
25	2A	6.4	25.5	25.8	195	6.1	14.5	4.54	.454	3.2	1.00	.100	67.7	75.8	740	23.1	18.4	5.75	.575	7.0	2.18	.218	1.09
26	2.25	7.1	NAC										93.4	97.5	1084	33.9	21.0	6.57	.657	8.2	2.56	.256	1.15
27	2.25A	7.1	No data										87.5	71.8	775	24.2	18.0	5.64	.564	8.3	2.59	.259	1.17
28	2.5	7.9	NAC										116	113	1495	46.8	25.0	7.81	.781	9.1	2.84	.284	1.14
29	2.5A	7.9	NAC										107.5	104	1585	48	20.5	6.42	.642	8.2	2.56	.256	1.04
30	2.75	8.7	NAC										61.4	61.5	626	19.6	19.0	5.95	.595	5.2	1.62	.162	0.597
31	2.75A	8.7	NAC										53.3	50.9	541	16.9	18.3	5.73	.573	4.8	1.5	.15	0.55
32	3	9.5	20.7	17.2	17.4	0.43							45	43	440	13.7	20	6.25	.625	4.2	1.31	.131	0.442
33	3.1	9.8											85	81	774	24.2	20	6.25	.625	8	2.5	.25	0.817
Spherical																						
34	1	3.18	No data										34	43.1	360	11.2	16.0	5.0	0.50	4.0	1.25	.125	1.26
35	1.5	4.75	18.6	17.9	139	4.3	13.5	4.2	.422	2.4	.75	.075	76.6	62.6	807	25.0	18.5	5.8	.58	5.6	1.75	.175	1.18
36	1.5A	4.75	25.1	19.2	176	5.5	13.4	4.2	.420	2.5	.78	.078	50.6	57.4	606	18.9	18.0	5.6	.56	5.0	1.57	.157	1.05
37	1.75	5.56	19.7	19.9	185	5.8	14.5	4.53	.453	2.0	.62	.062	70.4	76.4	836	26.1	19.0	5.9	.59	6.6	2.06	.206	1.18
38	1.75A	5.56	28.9	27.5	266	8.3	13.5	4.2	.422	2.8	.78	.075	64.6	65.1	568	17.7	15.7	4.9	.49	6.4	2.00	.20	1.15
39	2.3	7.3	15.7	14.3	156	4.9	14.5	4.53	.453	1.2	.37	.037	94.3	88.2	966	30.2	19.0	5.9	.59	7.6	2.38	.238	1.04
40	2.3A	7.3	NAC										94.0	97.7	1094	34.2	20.0	6.25	.625	7.9	2.47	.247	1.08
41	2.5	7.9	NAC										131.2	126.5	1700	53.0	24.0	7.5	.75	8.6	2.69	.269	1.09
42	2.5A	7.9	NAC										102.2	96.9	1075	33.6	21.0	6.6	.66	9.0	2.81	.281	1.14
43	2.75	8.68	19	26	188	5.9							50.0	53.0	540	16.9	18.0	5.6	.56	4.5	1.40	.140	0.52

APPENDIX A: (Cont'd) Crater data — Frozen silt, Fairbanks, Alaska.

Charge data			Apparent crater data										True crater data									
Shot no.	Depth (λ)	Depth (ft)	Area (ft²) N-S	Area (ft²) E-W	Vol (ft³)	Vol lb	Diam (ft)	Diam (λ)	Diam lb	Depth (ft)	Depth (λ)	Depth lb	Area (ft²) N-S	Area (ft²) E-W	Vol (ft³)	Vol lb	Diam (ft)	Diam (λ)	Diam lb	Depth (ft)	Depth (λ)	Depth lb	h_c/h_d
Spherical (Cont'd)																							
44	3.0	9.5	NAC										92.0	121.8	1289	40.3	22.5	7.3	.73	10.4	3.26	.326	1.10
45	3.0A	9.5	4	6.5	30	1.0							62.2	53.5	600	18.7	17.9	5.6	.56	6.0	1.88	.188	0.63
46	3.1	9.8	5.1	2	25	.8							40.0	25.0	229	7.2	14.0	4.4	.44	5.0	1.57	.157	0.59
47	3.25	10.3	83	10	59.6	1.9							17.0	16.0	120	3.8	12.5	3.9	.39	2.0	.62	.062	0.195
Wt = 8 lb H/D = 4																							
48	1	2	9.5	10.8	34.4	4.3	8.5	4.25	1.06	1.7	.85	.21	19.7	20.8	130.2	16.3	11.0	5.5	1.38	3.0	1.5	.375	1.5
49	1A	2	8.0	10.0	39.9	5.0	7.5	3.75	.94	2.3	1.15	.29	17.9	18.6	117.0	14.6	10.0	5.0	1.25	3.0	1.5	.375	1.5
50	1.5	3	11.3	8.3	47.4	5.9	7.7	3.85	.965	2.0	1.0	.25	17.4	20.2	110.0	13.8	10	5.0	1.25	3	1.5	.375	1.0
51	1.5A	3	Misfire																				
52	2	4	7.1	6.4	46.5	5.8	10	5.0	1.25	1	0.5	.125	25.8	28.0	180.2	22.6	13	6.5	1.62	4	2.0	.50	1.0
53	2A	4	NAC										32.6	31.0	204.0	25.5	12.5	6.25	1.56	4.8	2.4	.60	1.2
54	2.25	4.5	NAC										31.2	27.8	178.2	23.3	13.5	6.75	1.69	4.2	2.1	.525	.935
55	2.75	5.5	NAC										14.2	8.9	61.5	7.7	8.5	4.25	1.06	2	1.0	0.25	.362
56	2.75A	5.5	NAC										18.0	15.0	101.5	12.7	10.2	5.1	1.28	2.2	1.1	.275	.40
Spherical																							
57	1	2	10.7	9.9	48.7	6.1	8.4	4.2	1.05	2	1.0	.25	12.8	14.7	61.9	7.7	8	4.0	1.0	3	1.4	.375	1.5
58	1A	2	10.7	9.2	38.3	4.8	7.0	3.5	.865	2.3	1.15	.280	15.4	14.4	80.2	10.0	9	4.5	1.12	3.8	1.9	.475	1.9
59	1.5	3.0	11.5	13.6	61.0	7.6	7.8	3.9	.975	2.5	1.25	.312	16.9	16.2	81.4	10.2	8.6	4.3	1.07	3.4	1.7	.425	1.13
60	1.5A	2.0	Missing										20.8	16.9	90.4	11.3	9.0	4.5	1.12	3.6	1.3	.45	1.20
61	2	4.0	13.2	12.8	69.0	8.6	9.0	4.5	1.13	2.1	1.05	.263	24.0	25.2	142.0	17.8	10.4	5.2	1.30	4.3	2.15	.538	1.07
62	2A	4.0	13.9	15.1	83.6	10.4	9.7	4.85	1.21	2.4	1.2	.300	25.2	26.0	143.7	17.9	10.5	5.25	1.31	4.8	2.4	.60	1.2
63	2.25	4.5	4.1	11.3	52.0	6.5	9.0	4.5	1.13	1.3	1.15	.163	36.4	38.7	271.0	33.9	12.5	6.25	1.56	5.1	2.55	.638	1.13
64	2.25A	4.5	12.3	10.7	75.9	9.5	9.5	4.75	1.19	1.4	0.7	.175	38.6	39.6	318.0	39.8	14.6	7.3	1.82	4.4	2.2	.55	.98
65	2.5	5.0	2.9	3.6	8.5	1.1	3.4	1.7	.425	1.3	0.65	.163	25.8	22.8	169.0	21.5	12.9	6.45	1.61	3.4	1.7	.425	.68
66	2.5A	5.0	8.0	7.9	47.5	5.9	11.4	5.7	1.42	1.2	0.6	.15											
67	2.5B	5.0	.48	1.03	1.3	0.2							27.7	30.8	168.4	21.1	10.5	5.25	1.31	4.5	2.25	.562	.90
68	2.5C	5.0	NAC										31.2	34.2	213.1	26.6	12.5	6.25	1.56	4.8	2.4	.60	.96
69	2.75	5.5	NAC										7.2	8.9	27.5	3.4	7.1	3.55	0.925	1.8	0.9	.225	.327
70	2.75A	5.5	NAC										19.6	21.0	124.1	15.5	11.1	5.55	1.39	3,0	1.5	.375	.545
71	2.75B	5.5	7.8	9.3	44.9	5.6	8.2	4.1	1.02	1.7	0.85	.213	45.4	42.0	350.0	43.8	15.5	7.75	1.94	6.0	3.0	.75	1.09
Wt = 4 lb H/D = 4																							
72	1	1.6	6.34	6.57	27.3	6.8	7.1	4.44	1.77	1.6	1.0	0.4	9.5	8.6	33.6	8.4	6.8	4.25	1.7	2.5	1.57	.62	1.57
73	1A	1.6	4.6	4.4	15.7	3.9	6.0	3.75	1.5	1.3	0.82	0.32	9.6	9.9	38.5	9.64	6.5	4.08	1.63	2.6	1.62	.65	1.62
74	1.5	2.4	9.8	7.8	36.8	9.2	7.2	4.5	1.8	1.8	1.12	.45	16.1	13.8	67.2	16.8	8.0	5.00	2.0	3.2	2.0	.80	1.33
75	1.5A	2.4	7.3	6.3	25.4	6.4	6.2	3.88	1.55	1.6	1.0	0.4	12.5	11.5	53.1	13.3	7.0	4.38	1.50	3.2	2.0	.80	1.33
76	2	3.2	6.6	5.1	24.8	6.2	8.0	5.0	2.0	1.0	.625	0.25	18.9	19.2	96.8	24.2	8.8	5.5	2.2	3.7	2.32	.92	1.15
77	2A	3.2	6.2	6.4	28.9	7.2	8.0	5.0	2.0	1.2	.75	0.30	18.2	18.5	90.4	22.6	9.4	5.88	2.35	3.4	2.12	.85	1.06
78	2.25	3.6	6.6	5.3	28.2	7.1	8.0	5.0	2.0	1.1	.687	0.28	19.6	18.4	94.1	23.5	9.1	5.70	2.30	3.8	2.38	.95	1.05
79	2.25A	3.6	3.8	4.2	16.6	4.1	7.5	4.7	1.88	1.0	.625	0.25	25.5	23.0	127.2	31.8	9.3	5.8	2.35	4.5	2.80	1.12	1.25
80	2.5	4.0	1.4	3.7	6.6	1.6	3.5	2.18	.89	1.2	.75	0.30	23.6	23.2	138.4	34.7	9.6	6.0	2.40	4.4	2.75	1.10	1.10
81	2.5A	4.0	NAC										22.4	22.6	112.7	28.2	8.8	5.5	2.2	4.5	2.84	1.15	1.12
82	2.75	4.4	NAC										26.6	26.2	146.0	36.5	11.5	7.3	2.88	4.8	3.0	1.2	1.08
83	2.75A	4.4	CAMOFLET										CAMOFLET										
84	2.5B	4.0	NAC										27.8	29.8	191.5	48.0	13.0	8.2	3.25	3.4	2.13	.85	0.85
85	2.56	4.0	2.8	2.6	6.0	1.5	3.5	2.18	.89	1.0	.63	.25	26.6	23.7	167.0	41.8	12.5	7.9	3.2	4.1	2.68	1.02	1.02
86	2.75B	4.4	4.6	3.1	11.9	3.0	5.5	3.44	1.42	1.5	.945	.375	21.6	24.8	146.0	36.5	11.5	7.3	2.88	3.8	2.4	.95	0.865

APPENDIX A: (Cont'd) Crater data — Frozen silt, Fairbanks, Alaska.

Charge data			Apparent crater data										True crater data									
Shot no.	Depth (λ)	Depth (ft)	Area (ft²) N-S	Area (ft²) E-W	Vol (ft³)	Vol lb	Diam (ft)	Diam (λ)	Diam lb	Depth (ft)	Depth (λ)	Depth lb	Area (ft²) N-S	Area (ft²) E-W	Vol (ft³)	Vol .1b	Diam (ft)	Diam (λ)	Diam lb	Depth (ft)	Depth (λ)	Depth lb	h_c/h_d
Wt = 4 lb H/D = 4																							
87	2.75C	4.4	NAC										22.3	18.9	142.9	35.5	12.5	7.9	3.12	3.2	2.0	.80	0.73
88	2.9	4.6	NAC										8.3	6.7	34.8	8.7	8.5	5.35	2.12	2.6	1.64	.65	0.565
89	2.9A	4.6	NAC										7.2	11.4	68.5	17.1	10.5	6.6	2.63	2.7	1.70	.675	0.59
90	3.0	4.8	NAC										21.6	26.3	167.5	41.8	12.5	7.9	3.12	3.0	1.87	.75	0.625
91	3.0A	4.8	CRITICAL																				
92	3.1	4.9	CRITICAL																				
93	3.1A	4.9	CRITICAL																				
94	3.2	5.1	CRITICAL																				
95	3.2A	5.1	CRITICAL																				
96	3.3	5.25	NAC										4.8	6.9	26.7	6.7	7.5	4.7	1.87	1.1	.69	.275	0.21
97	3.3A	5.25	NAC										14.2	14.3	76.0	19.0	10.0	6.3	2.50	2.3	1.45	.575	0.44
98	3.5	5.6	NAC										10.0	10.6	76.0	19.0	11.5	7.2	2.87	1.3	.815	.375	0.23
99	3.5A	5.6	BELOW CRITICAL																				
100	3.7	5.9	BELOW CRITICAL																				
101	3.7A	5.9	BELOW CRITICAL																				
Spherical																							
102	1	1.6	4.6	5.2	17.0	4.2	5.5	3.44	1.42	1.2	.75	.30	10.0	9.4	38.4	9.6	6.5	4.1	1.62	2.2	1.38	.550	1.37
103	1A	1.6	6.9	6.2	22.3	5.6	6.2	3.9	1.55	1.8	1.12	.45	8.8	9.0	34.2	8.6	6.8	4.3	1.70	2.2	1.38	.550	1.37
104	1.5	2.4	7.6	8.4	29.8	7.4	6.3	3.95	1.58	1.9	1.20	.475	13.3	10.6	51.6	12.9	7.5	4.7	1.87	2.8	1.75	.70	1.17
105	1.5A	2.4	6.9	6.2	29.8	7.4	7.2	4.4	1.80	1.3	.815	.325	12.4	14.2	58.7	14.7	7.5	4.7	1.87	3.0	1.88	.750	1.25
106	2	3.2	8.1	6.1	31.6	7.9	6.7	4.2	1.70	1.4	.88	.350	23.1	19.4	119.5	29.9	9.7	6.05	2.42	3.7	2.32	.925	1.15
107	2A	3.2	4.9	5.1	22.3	5.6	6.5	4.08	1.62	1.0	.63	.25	19.1	18.3	90.9	22.7	8.3	5.2	2.08	3.6	2.26	.90	1.12
108	2.25	3.6	7.6	6.8	44.0	11.0	7.5	4.72	1.87	1.3	.815	.325	19.9	21.3	91.7	22.9	9.3	5.85	2.32	4.2	2.64	1.05	1.17
109	2.25A	3.6	NAC										29.4	22.3	147.2	36.9	9.3	5.85	2.32	4.4	2.76	1.1	1.22
Wt = 1 H/D = 4																							
110	1	1	2.6	1.7	6.28	6.28	4.2	4.2	4.2	0.6	0.6	0.6	4.8	4.6	14.1	14.1	4.7	4.7	4.7	1.5	1.5	1.5	1.5
111	1A	1	3.2	2.8	6.78	6.78	3.8	3.8	3.8	1.3	1.3	1.3	4.5	3.7	10.7	10.7	4.1	4.1	4.1	1.4	1.4	1.4	1.4
112	1B	1	2.7	2.2	5.56	5.56	3.9	3.9	3.9	1.0	1.0	1.0	2.9	3.6	7.4	7.4	4.0	4.0	4.0	1.4	1.4	1.4	1.4
113	1C	1	2.5	1.9	5.1	5.5	3.7	3.7	3.7	0.9	0.9	0.9	4.6	3.0	9.5	9.5	3.9	3.9	3.9	1.3	1.3	1.3	1.3
114	1.5	1.5	3.2	3.2	7.5	7.5	4.6	4.6	4.6	1.2	1.2	1.2	4.5	5.4	13.1	13.1	5.0	5.0	5.0	2.0	2.0	2.0	1.33
115	1.5A	1.5	3.3	3.2	8.3	8.3	4.3	4.3	4.3	1.1	1.1	1.1	5.6	5.1	16.0	16.0	5.2	5.2	5.2	1.8	1.8	1.8	1.20
116	1.5B	1.5	3.6	3.8	9.2	9.2	4.6	4.6	4.6	1.2	1.2	1.2	5.6	4.3	12.4	12.4	5.0	5.0	5.0	2.2	2.2	2.2	1.47
117	2	2	4.2	3.0	13.0	13.0	5.3	5.3	5.3	1.1	1.1	1.1	7.6	7.7	29.9	29.9	6.9	6.9	6.9	2.1	2.1	2.1	1.05
118	2A	2	3.9	3.5	10.7	10.7	5.2	5.2	5.2	1.1	1.1	1.1	8.6	8.1	28.6	28.6	5.7	5.7	5.7	2.3	2.3	2.3	1.15
119	2B	2	3.8	3.0	9.6	9.6	5.0	5.0	5.0	1.0	1.0	1.0	5.3	4.2	11.7	11.7	5.0	5.0	5.0	2.1	2.1	2.1	1.05
120	2.25	2.25	4.1	3.4	10.9	10.9	5.0	5.0	5.0	1.1	1.1	1.1	5.7	6.4	18.8	18.8	6.5	6.5	6.5	2.0	2.0	2.0	0.89
121	2.25A	2.25	2.7	3.2	11.4	11.4	6.0	6.0	6.0	0.7	0.7	0.7	12.2	10.0	48.4	48.4	7.3	7.3	7.3	2.6	2.6	2.6	1.15
122	2.25B	2.25	0.8	2.1	3.2	3.2	3.5	3.5	3.5	0.5	0.5	0.5	11.9	11.9	45.9	45.9	6.5	6.5	6.5	3.0	3.0	3.0	1.33
123	2.5	2.5	NAC										7.7	8.7	29.8	29.8	7.0	7.0	7.0	2.2	2.2	2.2	0.88
124	2.5A	2.5	3.9	4.4	17.3	17.3	7.0	7.0	7.0	0.8	0.8	0.8	11.1	8.2	35.0	35.0	7.0	7.0	7.0	2.7	2.7	2.7	1.08
125	2.75	2.75	2.5	2.4	4.1	4.1	3.7	3.7	3.7	1.2	1.2	1.2	2.8	3.2	6.6	6.6	4.0	4.0	4.0	1.6	1.6	1.6	0.58
126	2.75A	2.75	NAC										CAMOFLET										
127	2.95	2.95	NAC										CAMOFLET										
128	2.15	2.15	4.6	3.3	11.0	11.0	4.3	4.3	4.3	1.2	1.2	1.2	9.1	6.8	26.4	26.4	5.5	5.5	5.5	2.4	2.4	2.4	1.12
129	2.15	2.15	2.6	2.4	8.2	8.2	5.0	4.3	4.3	0.7	0.7	0.7	8.2	7.7	27.6	27.6	5.7	5.7	5.7	2.1	2.1	2.1	0.98

Table BI. Soil data, location 1.

Depth (ft)	Dry density (pcf)	Wet density (pcf)	Moisture content	Organic content	Description
2.0-3.55	41.2	77.5	113.0	9.1	Silt, brown, organic, frozen. At 2.4-2.55 ft, $\frac{1}{2}$-in. layers of pressed organic material and silt. Ice lenses, clear, hard, hairline thick, spaced hairline apart. Includes scattered ice lenses 1/16 in. thick from 2.0-2.55 and scattered $\frac{1}{8}$ in. ice lenses from 2.55 to 3.55 ft. Ice volume estimated 75%.
4.0-4.85	42.8	82.8	93.4		Silt, brown, organic, frozen. Hairline ice lenses hairline apart with scattered 1/16 in. ice lenses and one 3/16 in. ice lense at 5.15 ft. Scattered vertical ice lenses $\frac{1}{8}$ in. thick. Ice clear, hard, estimated volume 50%.
4.85-5.6	58.3	95.0	60.3		
5.6-6.05	11.9	56.9	379.5		Peat, dark-brown, frozen, well bonded, highly saturated. 10% visible ice.
6.05-6.65	29.5	73.6	157.3		Silt, organic, brown, frozen. Hairline ice lenses hairline apart with scattered 1/16 in. ice lenses, randomly oriented. Clear, hard. 50% by volume.
6.65-8.08	42.6	81.0	90.1	8.1	Silt, organic, brown, frozen. Ice lenses hairline, hairline distance apart. Scattered 1/16 in. ice lenses vertical and horizontal. 60% ice.
8.08-8.33	27.2	69.2	154.9		Peat, silty, frozen, well bonded. 20% visible ice.
11.5-12.2	84.4	107.7	34.5		Brownish-gray silt. No visible ice lenses. Frozen hard. Ice crystals—very few fine roots.
12.2-13.0	86.9	115.0	32.5		Gray silt. No visible ice lenses. Frozen hard.
13.0-14.0	84.4	112.6	33.2		Gray silt. No visible ice lenses. Microscopic ice. Well bonded.
14.0-14.65	82.8	112.5	36.1		Brownish gray silt. Frozen well bonded. No visible ice lenses. Very few fine roots.
15.1-15.6	93.1	120.0	28.9		Silt, greenish, frozen. Ice lenses 1/16 in. thick 2 to 4 in. apart. At 15.8 ft a cluster of $\frac{1}{4}$ in. hairline ice lenses spaced hairline apart. At 15.9 to 16.3 granular ice, clear, at one edge of core. Visible ice volume 15%.
15.6-15.85	90.9	116.8	28.8		
15.85-16.05	96.2	120.5	28.1		
16.05-16.15	-	-	29.8		
16.15-16.30	88.6	115.3	30.0	2.2	

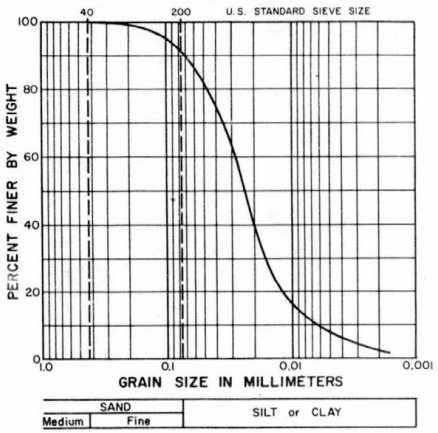

a. Depth: 2.00 to 3.55 ft.

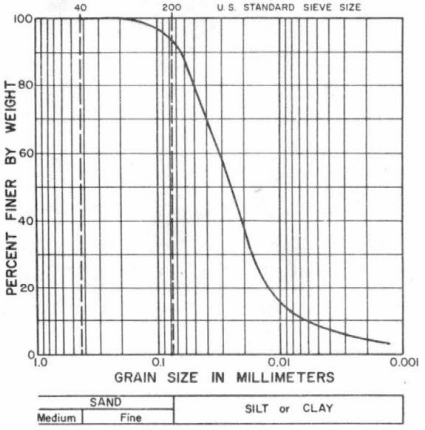

b. Depth: 4.0 to 4.85 ft.

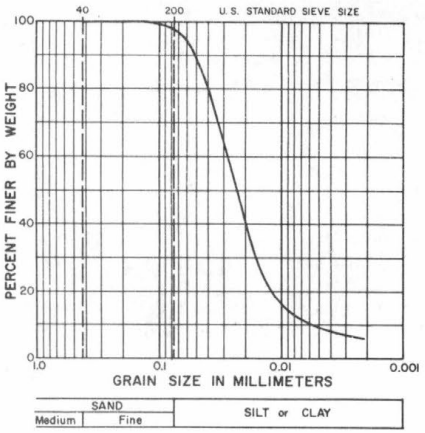

c. Depth: 4.85 to 5.6 ft.

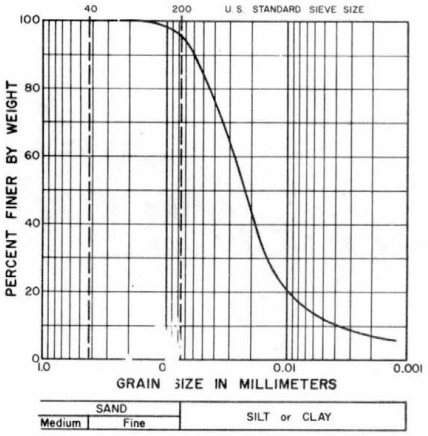

d. Depth: 6.05 to 8.05 ft.

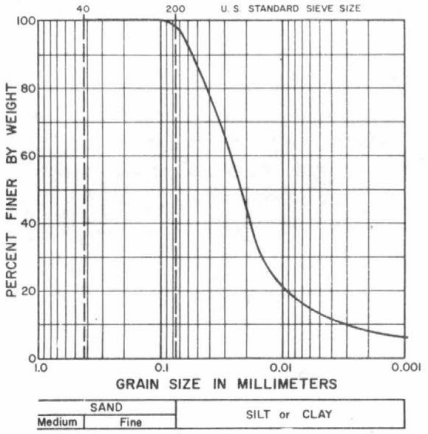

e. Depth: 15.08 to 16.25 ft.

Figure B1. Gradation curves, location 1.
(See Table BI for description.)

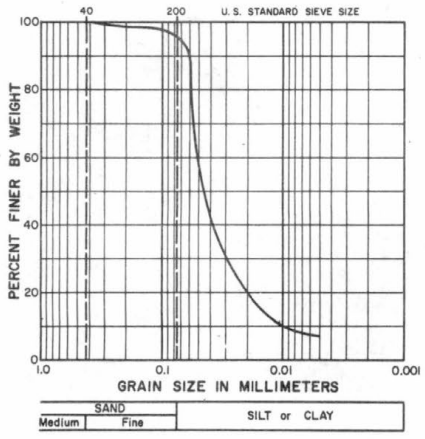

a. Depth: 3.5 to 4.5 ft. App. sp. gr. 2.69. Nat W. C. 321.8.

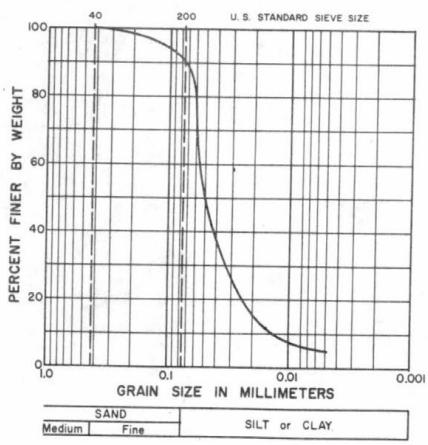

b. Depth: 8 to 8.75 ft. App. sp. gr. 2.59. Nat W. C. 159.2.

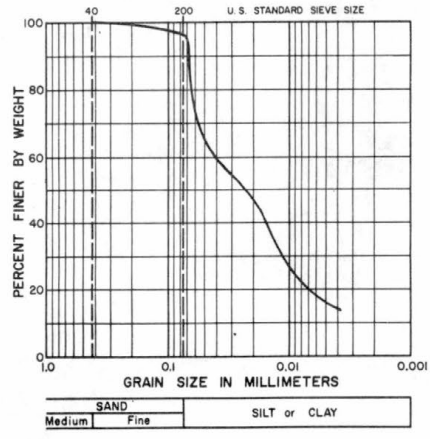

c. Depth: 11.25 to 12.5 ft. App. sp. gr. 2.74. Nat W. C. 56.3.

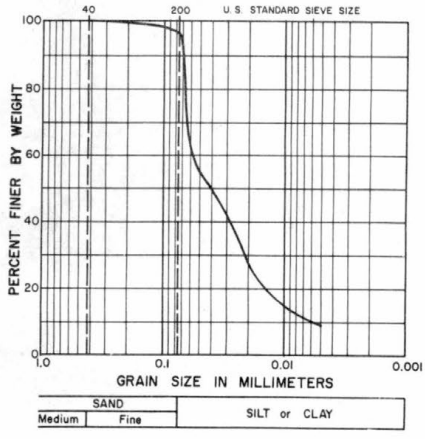

d. Depth: 14.5 to 15 ft. App. sp. gr. 2.75. Nat W. C. 24.8.

Figure B2. Gradation curves, location 2.

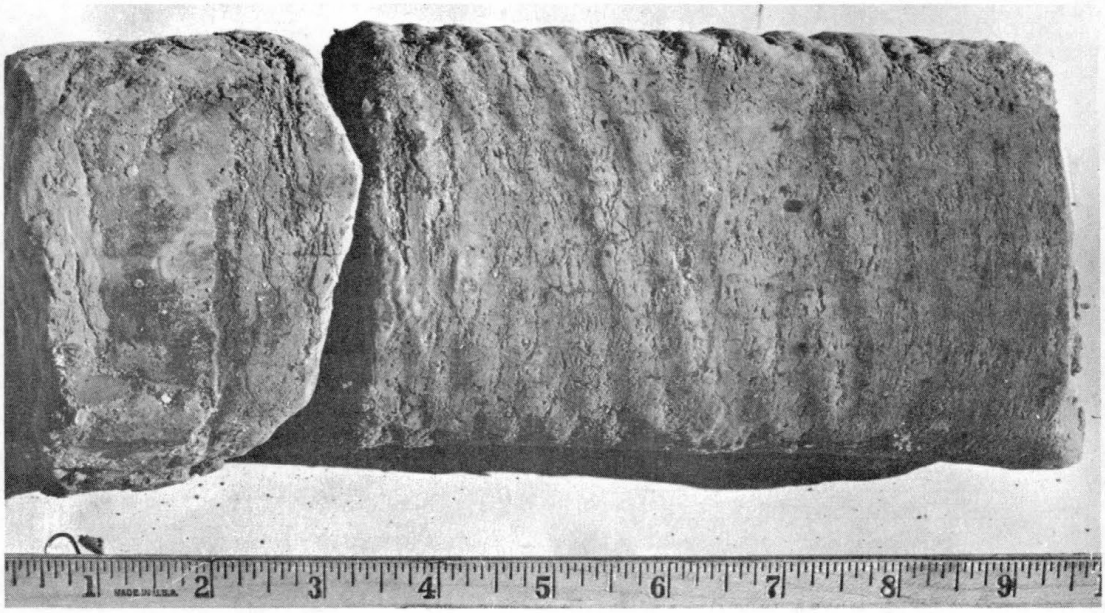

a. Depth 3.5 to 4.5 ft.

b. Depth 8.0 to 8.75 ft.

Figure B3. Typical core samples.

c. Depth 11.25 to 12 ft.

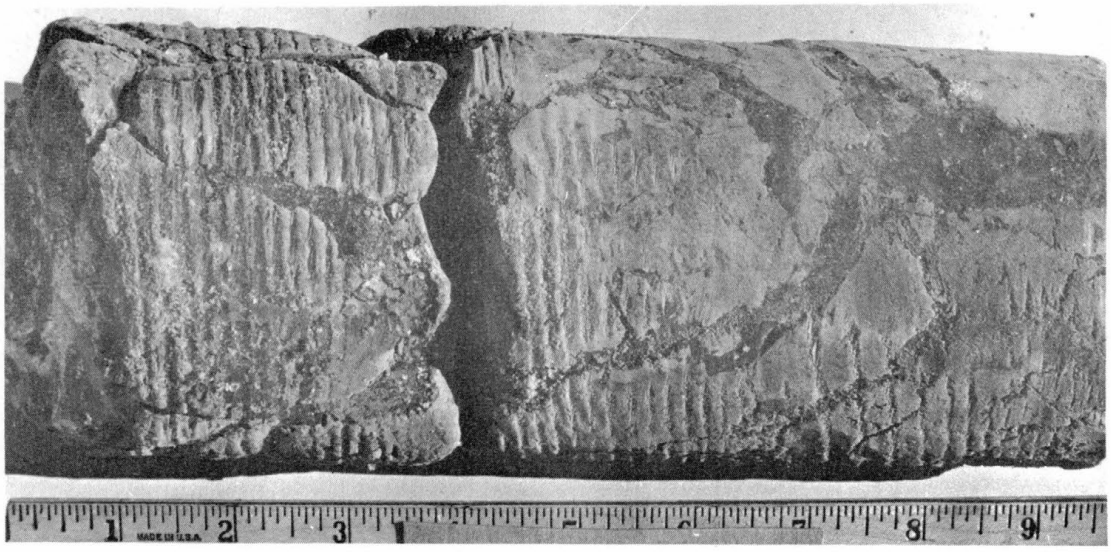

d. Depth 11.25 to 12 ft. Note random orientation of ice.

Figure B3 (Cont'd). Typical core samples.

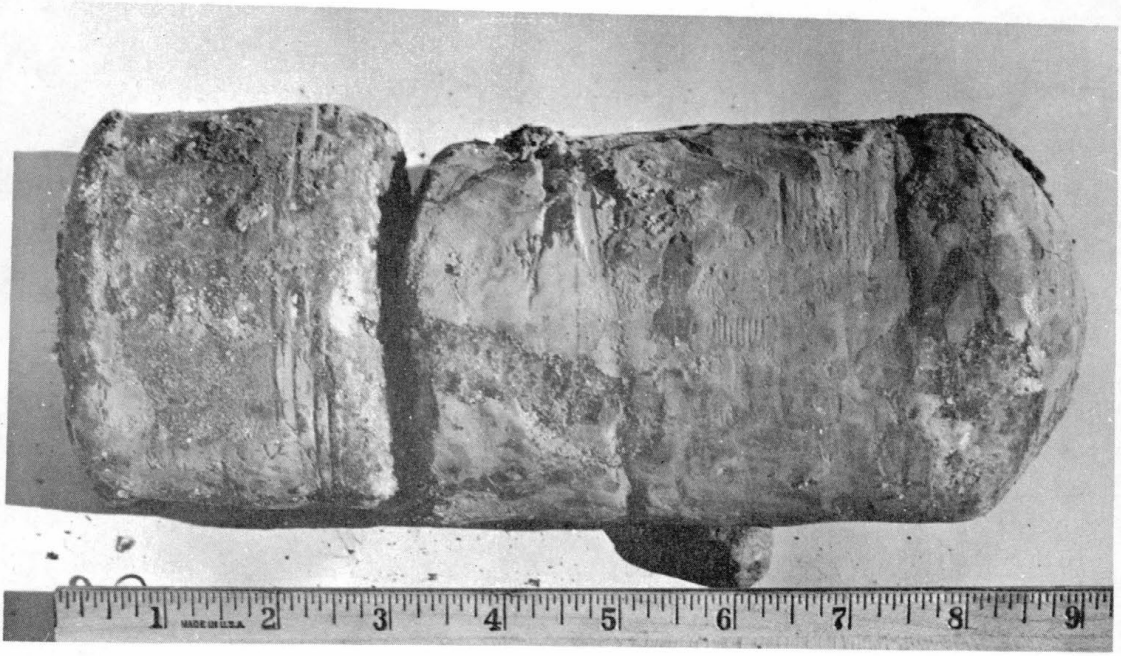

e. Depth 14.5 to 15 ft.

Figure B3 (Cont'd). Typical core samples.

APPENDIX C: CRATER DATA—GREENLAND SNOW AND ICE AND FROZEN SILT, CHURCHILL, ALASKA

(Data obtained by C. W. Livingston under contract to USA CRREL)

Table CI. Explosions in snow.
True crater data.

Shot no.	Wt (lb)	d_c, Depth of charge (ft)	(λ)	Vol/lb	h_c, Depth of crater (ft)	h_c/d_c
Atlas 60 percent straight gelatin dynamite						
1	2.5	1.36	1	49.4	3.4	2.5
2	2.5	0	0	14.4	2.0	∞
3	2.5	2	2.8	90.5	4.4	1.57
4	2.5	5.3	3.4	96.2	6.7	1.26
5	2.5	6.8	5	294	8.4	1.23
6	5.0	7.17	4.2	122	9.7	1.35
7	2.5	8.1	6	0	-	-
8	10	2.2	1	56	6.4	2.9
9	10	4.4	2	89	6.9	1.57
10	10	8.1	3.75	100	10.4	1.28
11	40	3.3	1	38	7.4	2.14
12	40	0	0	11.8	4.8	∞
13	40	6.8	2	54	10.1	1.46
14	40	12.5	3.65	71	16.6	1.33
15	2.5	1.36	1	19.5	1.7	1.35
16	2.5	2.7	2	45	3.8	1.4
17	2.5	5.4	3	99	6.8	1.25
18	10	2.2	1	22	2.9	1.32
19	10	4.3	2	39.4	6.08	1.41
20	10	8.6	4	107	10.4	1.27
21	10	10.7	6.25	0	-	-
22	10	5.4	3	48	7.7	1.43
23	10	3.2	1.875	44.6	5.7	1.78
24	2.5	4.1	3	75	5.4	1.32
25	10	6.5	3.8	84	9.06	1.4
26	2.5	4.1	3	62	4.8	1.17
27	10	6.5	3.8	74	8.7	1.34
28	40	10.3	3	71	13.5	1.36
29	10	2.2	1.25	53		
30	5	1.71	1	51		
31	2.5	9.6	7	0		
32	5	12.3	7.2	0		
33	10	2.2	1	0		
34	10	4.3	2	0		
35	20	11.5	4.3	0		
36	10	12.9	6	0		
37	10	15	7	0		
38	20	14	5.2	0		
39	40	20.5	6	0		
40	40	24	7	0		

Table C1 (Cont'd). Explosions in snow.

Shot no.	Wt (lb)	d_c, Depth of charge (ft)	(λ)	Vol/lb	h_c, Depth of crater (ft)	h_c/d_c
Military composition C-4						
1	2.5	1.3	1	54	3.9	3
2	2.5	0	0	9.4	1.9	∞
3	2.5	2.7	2	65	4.1	1.5
4	2.5	4.0	3	86	5.3	1.32
5	2.5	5.3	4	70	6.1	1.15
6	2.5	6.0	4.5	71	7.4	1.23
7	2.5	8.0	6	0	-	-
8	5.0	6.2	3.5	49	8.0	1.29
9	5.0	10.2	6	0	-	-
10	10.0	2.16	1	32	4.8	2.2
11	10.0	4.4	2	61	6.4	1.45
12	10.0	8.3	4	75	11.4	1.38
13	10.0	10.7	5	0	-	-
14	10.0	12.7	6	0	-	-
15	20.0	9.5	3.5	0	-	-
16	20.0	16.3	6	0	-	-
17	40.0	3.4	1	30	7.2	2.12
18	40.0	0	0	14.2	5.8	∞
19	40.0	6.8	2	44	9.6	1.4
20	40.0	11.4	3.3	43	16.4	1.32
21	40.0	20.7	6	0	-	-
22	10.0	6.5	3	98.4	8.4	1.3
23	40.0	10.2	3	44	13.2	1.3
24	10.0	2.15	1	46	5.3	2.5
25	5.0	1.7	1	52	4.3	2.5
Coalite 7S						
1	1	1	1	33	2.0	2
2	1		2	47	2.9	1.45
3			2	44	2.8	1.45
4			3	63	4.0	1.33
5			3.95	73	5.4	1.35
6			4.85	0	-	-
7			0	6.0	1.0	∞
8	2.5	1.33	1	36	3.1	2.31
9	2.5	2.5	2	50	4.2	1.68
10	2.5	5.2	3.8	67	6.8	1.3
11	5.0	5.65	3.3	0	-	-
12	2.5	6.3	4.6	1.01	.98	.015
13	2.5	7.3	5.35	0	-	-
14	2.5	0	0	8	1.6	∞
15	10	2.2	1	46	4.5	2.0
16	10	4.4	2	50	5.8	1.32
17	10	8.14	3.8	80.5	10.4	1.28
18	20	9.3	3.5	0	-	-
19	10	12.5	5.8	0	-	-
20	20	21.2	7.8	0	-	-
21	10	10.8	5	0	-	-
22	40	3.4	1	30	7.8	2.28
23	40	0	0	11	4.8	∞

Table C1 (Cont'd). Explosions in snow.

Shot no.	Wt (lb)	d_c, Depth of charge (ft)	(λ)	Vol/lb	h_c, Depth of crater (ft)	h_c/d_c
24	40	6.95	2	55	9.1	1.31
25	40	12.9	3.8	75	16.5	1.26
26	40	20.6	6	0	-	-
27	2.5	1.5	1	42	2.6	1.74
28	2.5	2.5	2	41	3.4	1.35
29	2.5	5.38	4	0	-	-
30	2.5	6.8	5	0	-	-
31	2.5	8.2	6	0	-	-
32	10	2.2	1	18	3.6	1.64
33	10	4.3	2	41	6.0	1.4
34	10	8.6	4	0	-	-
35	10	9.7	5	0	-	-
36	10	5.4	2.5	41.2	7.7	1.42
37	10	3.3	1.5	35	4.8	1.43
38	10	6.5	3	83	8.5	1.31
39	2.5	4.1	3	79	5.8	1.41
40	2.5	4.1	3	0	-	-
41	40	10.3	3	62	14.8	1.4
42	2.5	4.1	3	58	5.2	1.26
43	10	6.4	3	77	8.8	1.37
44	10	0	0	8.8		
45	10	2.2	1	38		
46	5	1.71	1	41		

Table CII. Explosions in ice.

Shot no.	Wt (lb)	d_c, Depth of charge (ft)	(λ)	Vol/lb	h_c, Depth of crater (ft)	h_c/d_c
Atlas 60 percent straight gelatin dynamite						
103	40	12.2	3.6	0	-	-
104	40	8.1	2.35	54.4	10	1.23
105	10	2.3	1	22.4	3.5	1.5
106	10	0.62	0.29	20.3	2.5	4.0
107	10	0.35	0.16	9.2	1.9	5.4
108	5	0.21	0.125	9.9	1.9	9.1
97	20	7.5	2.75	59	10	1.45
Military composition C-4						
1	5	1.2	.7	22.8	2	1.66
2	5	2.1	1.2	31	3.2	1.53
3	5	3.7	2.1	32	4.9	1.32
4	5	5.7	3.3	0	-	-
5	5	8.2	4.8	0	-	-
6	5	5.4	3.2	73	6.1	1.13
7	2.5	5.9	4.3	0	-	-
8	2.5	4.2	3.1	96	4.85	1.15
10	10	1.5	0.7	18	2.9	1.94
11	10	3.17	1.5	38	4.5	1.42

Table CII (Cont'd). Explosions in ice.

Shot no.	Wt (lb)	d_c, Depth of charge (ft)	(λ)	Vol/lb	h_c, Depth of crater (ft)	h_c/d_c
12	10	5.2	2.4	45	6.1	1.17
13	10	7.2	3.4	54	9.65	1.34
14	10	8.6	4	0	-	-
15	10	10.3	4.8	0	-	-
16	10	0.65	0.3	27	2.9	4.5
17	10	0.32	0.15	11	1.6	5.0
22	20	0.03	0	8	2.3	7.7
23	20	0.38	0.15	13	2.6	6.8
24	20	2.4	0.88	24	3.9	1.62
25A	20	2.9	1.1	26	4.6	1.58
25B	20	4.0	1.5	36	5.85	1.46
26	20	6.1	2.25	47	7.6	1.25
27	20	8.2	3	60	9.6	1.17
29	20	13	4.8	0	-	-
151	20	0.83	0.3	17	4.9	5.9
Coalite 5S						
30	25	0.23	0.017	7.4	0.95	
31	25	0.48	0.35	4.7	1.0	
32	25	1.3	1	12	1.65	
33	25	2.5	2	21	2.77	
34	25	4.4	3	25	2.75	
35	25	5.7	4	0	-	-
36	25	1.7	1.25	23	2.15	
37	25	1.1	0.8	11	1.6	
38	25	0.54	0.4	8	1.0	
39	25	3.4	2.5	70	3.9	
40	5	0.38	0.02	8.4	1.0	
41	5	1.0	0.6	14	1.95	
42	5	1.4	0.8	12	2.2	
43	5	3.5	2.0	25	3.8	
44	5	4.9	3.0	63	5.3	
45	5	6.9	4.0	0	-	-
46	10	0.44	0.02	6.6	1.8	
47	10	0.72	0.04	8	2.05	
48	10	1.4	0.65	26	2.6	
49	10	2.7	1	22	3.7	
50	10	6.1	3	68	6.2	
51	10	9.07	4	0	-	-
52	20	0.54	0.02	7.5	2.2	
53	20	0.93	0.04	10	2.2	
54	20	1.8	0.65	12	3.0	
55	20	3.7	1.25	25	5.0	
56	20	7.7	3.0	57	8.2	
57	20	11.4	4.0	0	-	-
60	5	0.32	0.2	13	1.4	4.4
61	5	0.51	0.3	12.7	1.8	3.5
62	5	1.5	1.0	23	2.4	1.6
63	5	2.5	1.5	44	3.5	1.4
64	5	3.8	2.0	55	4.4	1.16
65	10	0.49	0.02	14	3.0	6.1
66	10	0.92	0.04	18	4.0	4.4

Table CII (Cont'd). Explosions in ice.

Shot no.	Wt (lb)	d_c, Depth of charge (ft)	(λ)	Vol/lb	h_c, Depth of crater (ft)	h_c/d_c
67	10	1.7	0.8	19	2.8	1.55
68	10	3.4	1.5	28	4.1	1.2
69	10	7.0	3.0	19	8.4	1.2
70	5	10.0	6.0	0	-	-
71	5	8.1	5.0	0	-	-
72	10	9.9	4.5	70		
73	10	12.0	5.5	0	-	-
74	5	6.7	4.0	116	7.5	1.1
75	2.5	8.6	6.25	0	-	-
76	5	3.8	2.0	55	4.7	1.25
77	5	1.8	1.0	28	2.7	1.5
78	5	0.9	0.5	21.7	2.25	2.5
79	5	0.4	0.25	16	1.45	3.61
80	20	0.55	0.2	6.2	1.9	3.46
81	20	1.0	0.4	9.7	2.5	2.5
82	20	2.2	0.8	18.5	3.9	1.75
83	20	4.3	1.5	44.0	5.4	1.25
84	20	7.8	3.0	67	8.9	1.14
Coalite 7S						
85	5	7.3	4.5	0	-	-
86	10	9.7	4.5	0	-	-
87	2.5	6	4.5	0	-	-
88	2.5	4	3.0	72.4	4.4	1.1
89	20	12	4.5	0	-	-
90	5	5	3.0	68	5.2	1.04
120	10	6	3.0	106	7.2	1.2
Atlas 60 percent straight gelatin dynamite						
95	20	4	1.5	25	5.5	1.38
110	10	0	0	6.4	1.6	∞
113	10	1.2	2.5	14	2.2	1.85
115	10	5	4.5	50	5.6	1.1
116	10	7.6	3.0	92	8.7	1.15
A	2.5					
B						
C						
D	2.5					
E	2.5					
F	2.5					
G	2.5					
H	2.5	6.0		0	-	-
96	20	6.4	2.45	0	-	-
96R	20	6.1	2.25	32.1	8.8	1.45
98	20	12.0	4.4	0	-	-
99	20	9.0	3.3	84.1	9.5	1.05
100	20	10.1	3.8	97.2	11.2	1.1
101	40	14.5	4.2	0	-	-
102	40	-	-	0	-	-

Table CIII. Explosions in Churchill silt.

Shot no.	Wt (lb)	d_c, Depth of charge (ft)	(λ)	Vol (ft^3)	Vol/lb	h_c, Depth of crater (ft)	h_c/d_c
Atlas 60 percent straight gelatin dynamite							
1	2.0	1.9	1.5	13.3	6.7	2.67	1.4
2	2.0	1.8	1.5	13.3	6.7	2.48	1.38
3	2.0	1.9	1.5	13.5	6.8	2.4	1.27
4	2.0	1.9	1.5	18.8	9.4	2.3	1.21
5	2.0	1.9	1.5	18.7	9.3	7.75	1.45
6	2.0	1.8	1.5	17.4	8.7	2.46	1.37
7	2.0	1.8	1.5	11.1	5.5	2.65	1.47
8	2.0	1.9	1.5	15.0	7.5	2.52	1.33
9	2.0	1.8	1.5	14.4	7.2	2.55	1.42
10	2.0	1.8	1.5	12.1	6.0	2.75	1.45
11	2.0	1.8	1.5	15.1	7.5	2.67	1.47
12	2.0	1.8	1.5	15.8	7.9	2.62	1.47
13	2.0	2.0	1.6	N/A	-	2.71	1.69
14	2.0	2.0	1.6	26.4	13.2	2.66	1.33
15	2.0	2.2	1.75	40.4	20.1	2.74	1.25
16	2.0	2.0	1.6	28.7	14.3	2.34	1.17
17	2.0	2.1	1.65	45.2	27.6	2.66	1.27
18	2.0	2.1	1.65	36.4	18.2	2.59	1.23
19	2.0	2.7	2.2	16.0	8.0	-	-
20	2.0	3.1	2.5	2.0	1.0	0.76	0.24
21	2.0	3.6	2.9	0	0	-	-
22	0.5	0.8	1	3.7	7.4	1.15	1.44
23	0.5	1.1	1.4	5.6	11.2	1.51	1.37
24	0.5	1.3	1.7	7.7	15.4	1.70	1.30
25	0.5	1.6	2.0	12.0	24.0	2.04	1.28
26	0.5	1.8	2.2	0.48	0.96	1.2	0.67
27	0.5	2.1	2.7			-	-
28	1	1.0	1	5.2	5.2	1.45	1.45
29	1	1.2	1.2	9.5	9.5	1.67	1.46
30	1	1.4	1.4	8.6	8.6	1.86	1.33
31	1	1.7	1.7	18.0	18.0	2.15	1.25
32	1	1.9	1.9	19.0	19.0	2.33	1.23
33	1	2.2	2.2	21.3	21.3	2.56	1.16
34	1	2.4	2.4	31.7	31.7	2.72	1.13
35	1	2.6	2.6	0	0	-	-
36	1.9	1.0	0.8	10.1	5.0	1.58	1.58
37	1.9	1.2	1.0	12.6	6.2	1.68	1.4
38	1.9	1.4	1.1	17.4	8.6	2.17	1.55
39	1.9	1.7	1.4	22.3	11.1	2.37	1.4
40	1.9	2.0	1.6	17.6	18.8	2.56	1.28
41	1.9	2.0	1.6	26.3	13.2	2.54	1.27
42	1.9	2.3	1.8	54.1	27.2	3.63	1.32
43	1.9	2.6	2.1	50.0	25.0	3.37	1.3
44	1.9	3.0	2.4	30.2	15.1	3.31	1.10
45	1.9	3.3	2.6	1.8	0.9	1.89	0.57
46	4.75	1.6	1	31.8	6.8	2.34	1.46
47	4.75	1.9	1.1	35.7	7.5	2.89	1.52
48	4.75	2.1	1.25	34.6	7.1	2.84	1.35
49	4.75	2.5	1.5	48.6	10.1	3.53	1.41
50	4.75	3.0	1.8	67.5	14.2	3.13	1.04
51	4.75	3.4	2.0	99.7	21.0	4.15	1.32

Table CIII (Cont'd). Explosions in Churchill silt.

Shot no.	Wt (lb)	d_c, Depth of charge (ft)	(λ)	Vol (ft^3)	Vol/lb	h_c, Depth of crater (ft)	h_c/d_c
52	4.75	4.0	2.4	1.7	0.40	3.36	0.84
53	4.75	4.5	2.7	0	0	-	-
54	19.0	2.5	1	121.3	6.4	4.0	1.6
55	19.0	3.0	1.1	161.6	8.5	4.35	1.45
56	19.0	3.4	1.25	161.8	8.6	4.94	1.45
57	19.0	4.0	1.5	232.5	12.2	5.54	1.38
58	19.0	4.5	1.75	308.8	16.2	6.46	1.44
59	19.0	5.0	1.9	294.2	15.0	6.32	1.26
60	19.0	6.0	2.25	0	0	-	-
61	19.0	7.0	2.65	0	0	8.60	1.23
73	5	3.9	2.3	0	0	-	-
Military composition C-3							
62	2	1.0	0.7	0.4	0.2	1.6	1.6
63	2	1.3	1	15	7.5	2.3	1.77
64	2	1.5	1.2	11	5.5	2.1	1.4
64R	2	1.5	1.2	26.3	13	2.11	1.41
65	2	1.8	1.43	22.7	11.2	2.48	1.38
66	2	2.0	1.6	27.6	13.8	2.79	1.39
67	2	2.3	1.8	33	16.5	2.73	1.19
67R	2	2.2	1.75	36.5	18.2	2.88	1.31
68	2	2.5	2.0	28	14	3.04	1.21
68R	2	2.5	2.0	43	21.5	3.14	1.25
69	2	2.8	2.25	70	35	3.11	1.11
70	2	3.0	2.4	5.4	2.7	3.41	1.14
71	2	3.1	2.5	49	24.5	3.26	1.05
72	2	3.5	2.75	0	0	-	-
74	5	1.5	1	44.7	9.0	2.36	1.57
75	5	2.1	1.25	40	8.0	2.89	1.37
76	5	2.6	1.5	65	13	3.47	1.33
77	5	3.1	1.75	75.3	15.1	3.72	1.2
78	5	3.6	2.0	69.2	13.8	2.72	0.75
79	5	3.9	2.25	13.9	2.75	1.55	0.40
80	5	4.5	2.60	10.8	2.1	1.28	0.28
81	-	-		-	0	-	-
82	0.5	0.6	0.7	3.3	6.6	0.95	1.58
83	0.5	0.63	0.72	4.8	9.6	1.06	1.68
84	0.5	0.71	0.9	3.7	7.4	0.99	1.39
85	0.5	0.76	1.0	3.5	7.0	0.96	1.26
86	0.5	0.92	1	3.3	6.6	1.2	1.30
87	0.5	0.98	1.25	5.7	11.4	1.31	1.33
88R	0.5	1.16	1.5	5.9	11.8	1.53	1.32
89	0.5	1.5	1.75	11.5	23	1.99	1.33
90	0.5	1.6	2.0	9.5	19	1.97	1.23
91	0.5	1.9	2.25	1.7	3.4	2.18	1.15
92	0.5	2.0	2.5	1.0	2.0	2.45	1.22
93	0.5	2.2	2.75	0.47	1.0	2.56	1.13
94	1.0	0.73	0.73	6.2	6.2	1.28	1.75
95	1.0	1.1	1.1	11.5	11.5	1.66	1.5
96	1.0	1.4	1.4	8.7	8.7	1.70	1.21
97	1.0	1.8	1.8	17.7	17.7	2.34	1.36

Table CIII (Cont'd). Explosions in Churchill silt.

Shot no.	Wt (lb)	d_c, Depth of charge (ft)	(λ)	Vol (ft^3)	Vol/lb	h_c, Depth of crater (ft)	h_c/d_c
98	1.0	2.3	2.3	0.76	0.76	2.81	1.22
99	1.0	2.5	2.5	1.4	1.4	3.08	1.23
100	1.0	2.8	2.8	0.3	0.3	3.38	1.2
101	20	2.8	1.0	3.06	0.15	3.43	1.23
102	20	3.3	1.25	-	-	-	-
103	20	1.0	0.38	68.8	3.4	2.24	2.24
104	20	1.5	0.55	94	4.7	3.14	2.2
105	20	2.1	0.75	106	5.3	3.35	1.6
106	20	2.6	1.0	175	8.7	4.19	1.6
107	20	3.0	1.1	208	10.4	4.53	1.51
108	20	3.6	1.25	287	14.3	5.09	1.41
109	20	4.1	1.5	275	13.7	5.45	1.33
110	20	4.5	1.65	354	17.7	5.90	1.31
111	20	5.0	1.85	459	22.9	6.39	1.27
112	20	5.5	2.0	647	32.4	6.68	1.21
113	20	6.0	2.2	0	0	-	-
114	20	7.2	2.65	0	0	-	-
Coalite 7S							
115	2			-		-	-
115R	2	.95	.9	18.5	9.2	1.82	1.92
116	2			-		-	-
116R	2	1.09	1	17.6	8.8	1.83	1.68
117	2	1.4	1.1	12.9	6.9	1.88	1.34
118	2	1.6	1.25	21.9	10.9	2.30	1.44
119	2	1.8	1.5	23.8	11.9	2.56	1.42
120	2	2.1	1.65	32.5	16.2	2.75	1.30
121	2	2.3	1.8	48.2	24.1	3.23	1.4
122	2	2.7	2.15	42.6	21.3	3.25	1.2
123	2	2.4	1.9	4.3	2.1	3.27	1.36
124	2	2.9	2.3	3.7	1.8	3.69	1.27
125	-	-	2.38			-	-
126	5	3.0	1.75	0	0	-	-
127	5	3.2	1.85	76.8	15.36	4.15	1.3
128	5	3.5	2.0	20.1	4.02	4.47	1.28
129	5	3.8	2.25	0.85	0.17	1.57	0.41
130	-	-		-	-	-	-
131	-	-		-	-	-	-
132	-	-		-	-	-	-
133	5	1.7	1	43.2	8.6	2.47	1.45
134	5	1.8	1	36.0	7.2	2.77	1.54
135	5	2.0	1.15	41.1	8.2	2.96	1.45
136	5	2.3	1.35	49.9	10.0	3.31	1.44
137	-	-	-	-	-	-	-
138	-	-	-	-	-	-	-
139	-	-	-	-	-	-	-
140	20	1.8	0.72	87.1	43	3.39	1.88
141	20	2.5	1	140.8	7.0	3.94	1.57
142	20	3.0	1.1	253.9	12.6	4.65	1.55
143	20	3.5	1.3	229.9	11.4	4.40	1.25
144	20	4.1	1.5	167.3	8.3	4.57	1.11

Table CIII (Cont'd). Explosions in Churchill silt.

Shot no.	Wt (lb)	d_c, Depth of charge (ft)	(λ)	Vol (ft^3)	Vol/lb	h_c, Depth of crater (ft)	h_c/d_c
145	20	4.4	1.6	293.4	14.6	5.17	1.18
146	20	4.2	1.55	240	12.0	5.56	1.33
147	20	5.2	1.9	355	17.3	5.87	1.13
148	20	5.6	2.1	419	20.9	6.93	1.24
149	20	7.0	2.6	0	-	-	-
150	20	6.4	2.4	241	12.1	7.27	1.14
151	20	7.2	2.65	0	-	-	-
152	20	8.0	2.9	0	-	-	-